Oil & Gas Science and Technology – Rev. IFP Energies nouvelles, Vol. 66 (2011), No. 5, pp. 801-822

DOI: 10.2516/ogst/2011116

Dossier

R&D for Cleaner and Fuel Efficient Engines and Vehicles
R&D pour des véhicules et moteurs plus propres et économes

Spray Atomization Models in Engine Applications, from Correlations to Direct Numerical Simulations

F. Dos Santos and L. Le Moyne

ISAT Université de Bourgogne, 49 rue Mlle Bourgeois, 58000 Nevers - France
e-mail: fabien.dos-santos@u-bourgogne.fr - luis.le-moyne@u-bourgogne.fr

Résumé — Modèles de spray dans les applications moteur, des corrélations aux simulations numériques directes — Les sprays sont parmi les principaux facteurs de qualité, dans la formation du mélange et la combustion, dans un grand nombre de moteurs (à combustion interne). Ils sont de toute première importance dans la formation de polluants et l'efficacité énergétique, bien qu'une modélisation adéquate soit encore en développement. Pour un grand nombre d'applications, la validation et la calibration de ces modèles demeurent une question ouverte. Aussi, présentons-nous un aperçu des modèles existants et proposons quelques voies d'amélioration. Les modèles sont classés en non-dimensionnels et dimensionnels allant de formules simples dédiées à des applications proches du temps réel à des descriptions détaillées des premiers stades de l'atomisation.

Abstract* — *Spray Atomization Models in Engine Applications, from Correlations to Direct Numerical Simulations — *Sprays are among the very main factors of mixture formation and combustion quality in almost every (IC) engine. They are of great importance in pollutant formation and energy efficiency although adequate modeling is still on development. For many applications, validation and calibration of models are still an open question. Therefore, we present an overview of existing models and propose some trends of improvement. Models are classified in zero dimensional and dimensional classes ranging from simple formulations aimed at close-to-real-time applications to complete detailed description of early atomization stages.*

INTRODUCTION

Spray applications range from large scale dispersion of insecticides to nanometer thin film deposits with ion sources. What they have in common is the transformation of a continuous phase (mostly liquids) into a number of separated droplets created by a specific device, or atomizer. For characterization of sprays, the most commonly used qualities are size/number distribution of droplets, penetration and spray angle. Atomizers technologies are based on a number of principles that achieve break-up of continuous phase with surface or volume forces. The main forces used and their corresponding atomizers used in injection applications for engines are listed non-exhaustively in Table 1.

TABLE 1

Main types of forces and corresponding atomizers

Force	Atomizer type
Inertial	Rotating, vibration, impinging, swirl type, etc.
Aerodynamic drag	Pressure hole, swirl, two-fluid, air-assisted, etc.
Gas bubbles growth/collapse	Pressure hole, cavitation, flash, effervescent, void, etc.

The cost of calibration of the many parameters to be optimized in modern engines renders real engine tests prohibitively high. It is therefore a need to develop effective models able to give a description of mechanisms with a less cost. Simple 0D models are currently integrated into complete phenomenological engine models able to find, through optimization algorithms, ensembles of parameter values that comply with pollutant regulations and fuel efficiency for a number of functioning conditions. 1D to 3D models are used in design tasks at every stage of engine development.

In the last years, intensive use of CFD (Computational Fluid Dynamics) codes in engines has still increased and generalized. Yet, among the features needed for more effective models, there is the atomization and spray sub-models of many engine models. From pioneering work (Wakuri *et al*., 1960; Dent, 1971; Hiroyasu *et al*., 1978) on penetration correlations to recent efforts in LES and DNS modeling (Apte *et al*., 2003; De Villiers *et al*., 2004; Menard *et al*., 2005; Fuster *et al*., 2009; Lebas *et al*., 2009), spray models expand through a very large range of concepts. It is our aim to have an overview of existing tools for modeling and prospective insight of future techniques. We focus our interest in the liquid and droplet treatment on a surrounding gas, putting aside evaporation and mixing models which we consider as out of scope of this paper.

First we list non-dimensional models and correlations for spray penetration, spray angle, liquid length and characteristic drop size. In this category, we include atomization models for primary and secondary break-up as their results do not depend on space coordinates, although in order to obtain those results dimensional equations must be solved (Le Moyne, 2010).

1 0D MODEL

Most of the investigations on sprays conclude with empirical or semi-empirical laws, which predict the characteristics of the spray as a function of several parameters.

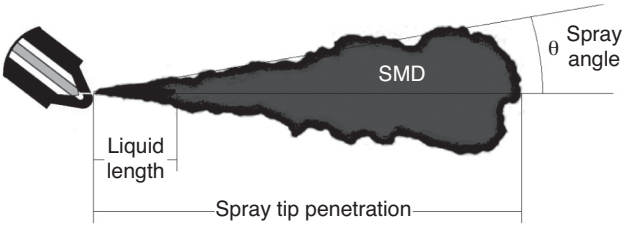

Figure 1

Different spray parameters.

A spray can be roughly described by four parameters *(Fig. 1)*: the spray tip penetration S, the spray angle θ, the break-up length L_b (or liquid length) and the global Sauter mean diameter $\bar{x}_{32}$. All together are related in the process of disintegration of the spray and can be modeled by 0D models. Other parameters, like air entrainment which results from the spray, won't be analyzed in this study. Also, according with the data, the models are for hole injectors.

1.1 Spray Angle Models

Spray angle (defined in *Fig. 1*) is influenced by the injector characteristics, fuel properties and ambient conditions. Basically during injection, the angle increases rapidly, reaches a maximum and then decreases to reach a constant value (Lefebvre, 1989). Many authors try to assess and calculate to give the constant value for the spray angle. The collected 0D spray angle models are shown in Table 2.

1.1.1 Reitz and Bracco Model

Reitz and Bracco (1979) proposed a model for the spray angle by employing the aerodynamic break-up model of Ranz (1958). It includes the ratio of Reynolds and Weber numbers of the liquid flow in the function $f(\gamma)$:

$$\tan(\theta) = \frac{4\pi}{A}\left(\frac{\rho_g}{\rho_l}\right)^{0.5} f(\gamma) \quad (1)$$

TABLE 2

Different correlations for spray angle

Model	Correlation	References
Reitz and Bracco	$\tan(\theta) = \frac{4\pi}{A}\left(\frac{\rho_g}{\rho_l}\right)^{0.5} f(\gamma)$	Reitz and Bracco, 1979
Reitz and Bracco Simplified	$\tan(\theta) = \frac{4\pi}{A}\left(\frac{\rho_g}{\rho_l}\right)^{0.5} \frac{\sqrt{3}}{6}$	Heywood, 1988
Ruiz and Chigier	$\tan(\theta) = \frac{4\pi}{A}\left(\frac{\rho_g}{\rho_l}\right)^{0.5} f(\gamma)\left(\frac{Re_l}{We_l}\right)^{-0.25}$	Ruiz and Chigier, 1991
Arai	$\theta = 0.025\left(\frac{\rho_g \Delta P d_o^2}{\mu_g^2}\right)^{0.25}$	Arai *et al*., 1984
Hiroyasu and Arai	$2\theta = 83.5\left(\frac{l_o}{d_o}\right)^{-0.22}\left(\frac{d_o}{d_{sac}}\right)^{0.15}\left(\frac{\rho_g}{\rho_l}\right)^{0.26}$	Hiroyasu and Arai, 1990
Arrègle	$\tan(\theta) = d_o^{0.508} P_{inj}^{0.00943} \rho_g^{0.335}$	Arrègle *et al*., 1999
Siebers	$\tan(\theta) = C_\theta\left[\left(\frac{\rho_g}{\rho_l}\right)^{0.19} - 0.0043\left(\frac{\rho_l}{\rho_g}\right)^{0.5}\right]$	Siebers, 1999

where ρ_g and ρ_l are the gas and liquid density, respectively. A is a constant depending on the nozzle design and may be extracted from experiments or approximated by Equation (2):

$$A = 3.0 + 0.28\left(\frac{l_o}{d_o}\right) \tag{2}$$

where d_o is the nozzle diameter and l_o the length of the nozzle hole. $f(\gamma)$ is a weak function of the physical properties of the liquid and the injection velocity:

$$f(\gamma) = \frac{\sqrt{3}}{6}\left(1 - e^{(-10\gamma)}\right) \tag{3}$$

$$\gamma = \left(\frac{Re_l}{We_l}\right)^2 \frac{\rho_l}{\rho_g} \tag{4}$$

where Re_l and We_l are the Reynolds number and the Weber number respectively, based on liquid properties and nozzle diameter:

$$Re_l = \frac{\rho_l V_{inj} d_o}{\mu_l} \tag{5}$$

$$We_l = \frac{\rho_l V_{inj}^2 d_o}{\sigma_l} \tag{6}$$

$$V_{inj} = C_v\sqrt{\frac{2\Delta P}{\rho_l}} \tag{7}$$

where V_{inj} is the injection velocity, C_v the velocity coefficient, μ_l the liquid dynamic viscosity, σ_l the surface tension of liquid and ΔP the difference between injection pressure and ambient pressure.

1.1.2 Reitz and Bracco Simplified Model

Heywood (1988) simplified Equation (3) into Equation (1) for cases with high-pressure sprays because the liquid warms and his viscosity decreases. In these cases, $f(\gamma)$ becomes asymptotically equal to $3^{1/2}/6$ because of the rise of γ. These operating conditions can be found in most of modern Diesel injectors:

$$\tan(\theta) = \frac{4\pi}{A}\left(\frac{\rho_g}{\rho_l}\right)^{0.5} \frac{\sqrt{3}}{6} \tag{8}$$

1.1.3 Ruiz and Chigier Model

Ruiz and Chigier (1991) examined the previous aerodynamic break-up model and suggested a modification based on injection parameters atypical of modern Diesel engines:

$$\tan(\theta) = \frac{4\pi}{A}\left(\frac{\rho_g}{\rho_l}\right)^{0.5} f(\gamma)\left(\frac{Re_l}{We_l}\right)^{-0.25} \tag{9}$$

1.1.4 Arai Model

Arai *et al*. (1984) gave the following equation in order to determine the spray angle:

$$\theta = 0.025\left(\frac{\rho_g \Delta P d_o^2}{\mu_g^2}\right)^{0.25} \tag{10}$$

where ρ_g is the gas density, ΔP the difference between fuel injector pressure and ambient gas pressure, d_o the nozzle diameter, and μ_g the gas dynamic viscosity.

1.1.5 Hiroyasu and Arai Model

Hiroyasu and Arai (1990) have proposed an empirical equation for the spray angle which includes some characteristics of the nozzle:

$$2\theta = 83.5\left(\frac{l_o}{d_o}\right)^{-0.22}\left(\frac{d_o}{d_{sac}}\right)^{0.15}\left(\frac{\rho_g}{\rho_l}\right)^{0.26} \tag{11}$$

where l_o is the length of the nozzle, d_o the diameter of the nozzle, and d_{sac} the diameter of the sack chamber. All these parameters are intrinsic characteristics of injector used.

1.1.6 Arrègle Model

Arrègle *et al*. (1999) used a simple equation with different coefficients which have been fitted with experimental results on a Diesel spray. This equation depends only of the nozzle

diameter, the injection pressure and the gas density. Equation (12) is the result:

$$\tan(\theta) = d_o^{0.508} P_{inj}^{0.00943} \rho_g^{0.335} \quad (12)$$

where P_{inj} is the injection pressure. We can see that the spray angle does not depend on injection pressure because the exponent is very small. This is in agreement with some other models.

1.1.7 Siebers Model

Siebers (1999) has suggested a model in which the spray angle depends on the liquid and gas densities, and a constant:

$$\tan(\theta) = C_\theta \left[\left(\frac{\rho_g}{\rho_l} \right)^{0.19} - 0.0043 \left(\frac{\rho_l}{\rho_g} \right)^{0.5} \right] \quad (13)$$

where C_θ is a coefficient depending on the injector characteristics.

1.1.8 Analysis and Validation

In order to compare the previous models, experimental data with high-pressure injectors has been used (from Sandia (2010)'s online database). The 0D results are compared to the measured experimental data. The fuel is the Phillips research grade DF2 fuel (ρ_l = 699 kg/m^3 at T_l = 450 K). Experimental and simulated values are considered for three different nozzle diameters, whose characteristics are shown in Table 3.

TABLE 3

Characteristics of nozzles

Orifice diameter	Discharge coefficient	Area-contraction coefficient	Velocity coefficient	Length-to-diameter
d_o (mm)	C_d	C_a	C_v	l_o/d_o
0.185	0.64	0.93	0.68	5.4
0.241	0.71	0.92	0.77	4.2
0.33	0.66	0.89	0.74	3.0

The ambient temperature T_g is set to 300 K for diameter 0.330 mm and 450 K for diameters 0.241 and 0.185 mm (non-vaporizing experiments). The percentage of oxygen is set to 0%, in order to disable combustion.

Experimental data show that the injection pressure doesn't seem to influence the spray angle value *(Fig. 2)*. This has been observed as well by Arrègle *et al.* (1999), resulting in a tiny injection pressure exponent in equation 12 (0.00943, while exponent for nozzle diameter is 0.508 and exponent for ambient density is 0.335, proving that the injection pressure does not really affect spray angle). Considering that, many spray models don't take into account the injection pressure in their equations.

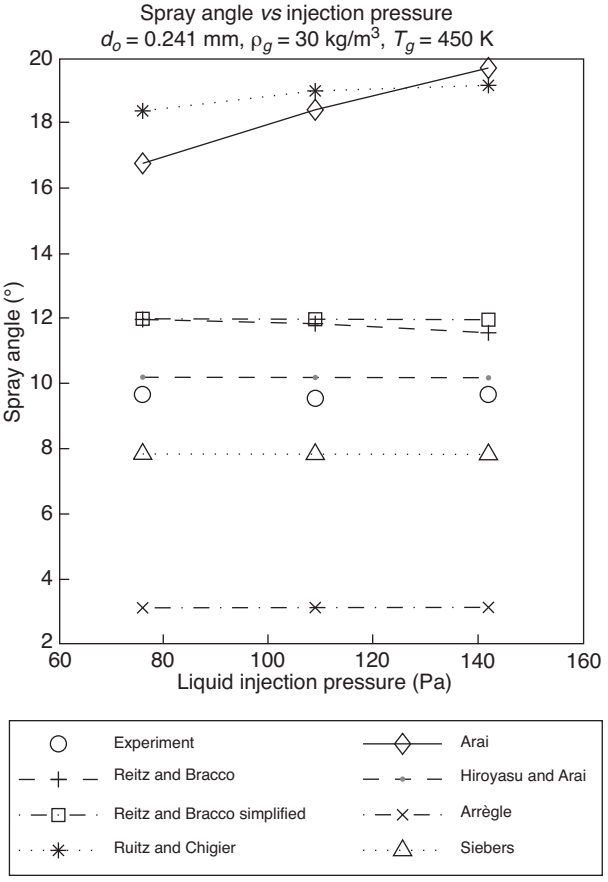

Figure 2

Evolution of spray angle with the injection pressure.

Some other models show an evolution in Figure 2 because the injection pressure is indirectly included in their equation. For example in Arai model with the term ΔP and in Ruiz and Chigier and Reitz and Bracco models with Reynolds and Weber numbers.

As discussed in (Siebers, 1999), Appendix A, the only parameter that seems to have a clear influence on spray angle, apart from the injector orifice characteristics, is the ambient gas to fuel density ratio. Thus, for a given fuel, the parameter of interest is the ambient density. Experimental data *(Fig. 3)* show a rise of the spray angle when the ambient density increases.

It can be noted that Reitz and Bracco, and Reitz and Bracco Simplified models are similar in the cases with low ambient densities but not after. In fact when the ambient density increases, the first term $(Re_l/We_l)^2$ in the gamma function rises a bit because of the change of the injection velocity, but gamma value is much more influenced (in our case) by the second term ρ_l/ρ_g, which reduces faster. Consequently,

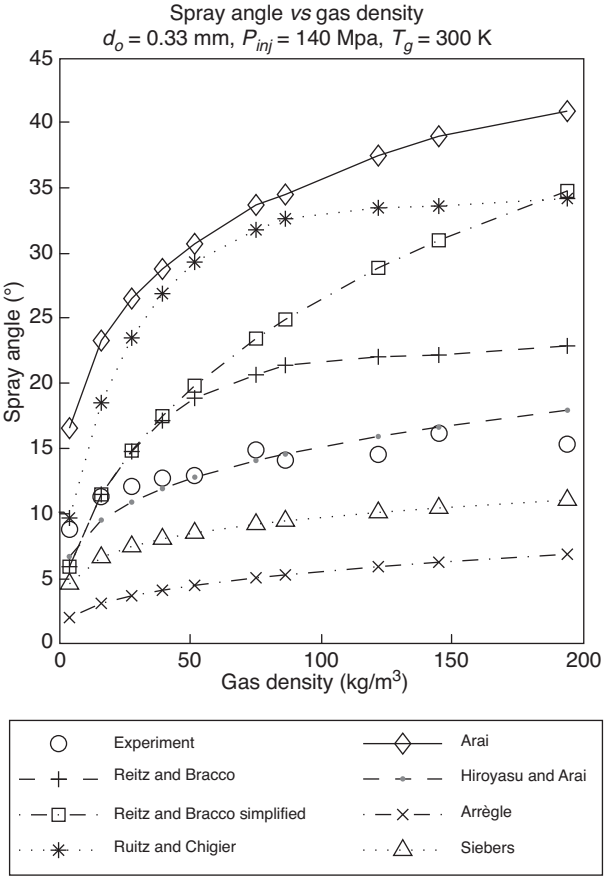

Figure 3

Evolution of the spray angle with the ambient density.

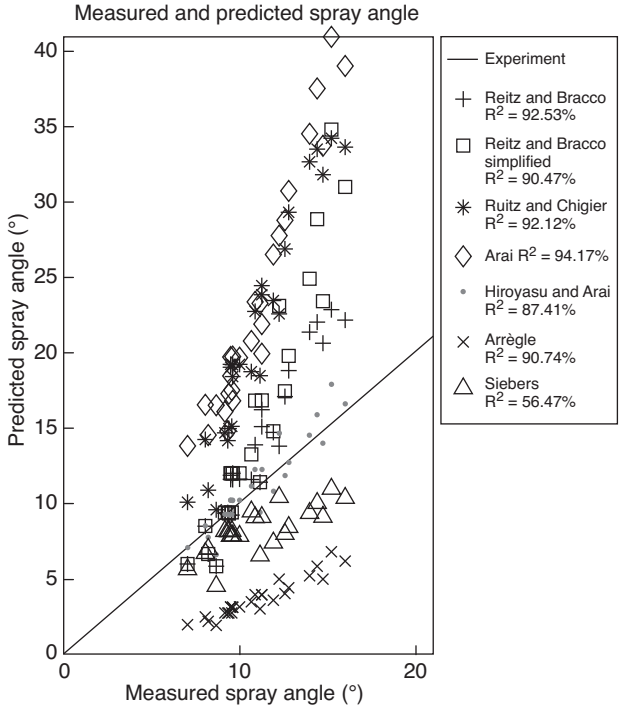

Figure 4

Comparison between measured and predicted spray angle.

gamma decreases and $f(\gamma)$ is no longer equal to $3^{1/2}/6$. Another variable which can change considerably the value and the evolution of $f(\gamma)$ is the fuel temperature. When it increases, the fuel viscosity μ_l decreases a lot, and changes the Reynolds number. The term $(Re_l/We_l)^2$ increases and becomes more significant than ρ_l/ρ_g. In this case (high fuel temperature), both models should be equal (because $f(\gamma) \approx 3^{1/2}/6$).

In Figure 4 are represented 27 points with at least one different characteristic between each other (ambient density, injection pressure, nozzle diameter...). The coefficient of determination R^2 shows a good correlation between models and experimental data. Concerning Siebers model, our values chosen for the constant C_θ don't seem to be adapted to the injectors used for this study, but the evolution on spray angle for a selected injector is well represented *(Fig. 3)*.

The coefficient of determination and the mean absolute percentage error for each model are given in Table 4 (the best values are in bold). In our case, Hiroyasu and Arai gives a spray angle value closed to the measured one but its prediction on the evolution of the spray angle is not really good. On the contrary, Arai model has a good correlation with the experimental data, but must be calibrated in order to give values close to the measured spray angle.

TABLE 4

Comparison results between models and data

Spray angle model	Coefficient of determination	Mean absolute percentage error
Reitz and Bracco	92.53%	23.91%
Reitz and Bracco simplified	90.47%	38.21%
Ruiz and Chigier	92.12%	87.85%
Arai	**94.17%**	106.57%
Hiroyasu and Arai	87.41%	**7.15%**
Arrègle	90.74%	67.69%
Siebers	56.47%	24.27%

1.2 Spray Tip Penetration Models

The knowledge of spray tip penetration is important in design of Diesel and Gasoline Direct Injection (GDI) engines. The

TABLE 5

Different correlations for spray tip penetration

Model	Correlation	References
Wakuri	$S = 1.189 C_a^{0.25} \left(\frac{\Delta P}{\rho_g}\right)^{0.25} \left(\frac{d_o t}{\tan(\theta)}\right)^{0.5}$	Wakuri *et al*., 1960
Dent	$S = 3.07 \left(\frac{\Delta P}{\rho_g}\right)^{0.25} (d_o t)^{0.5} \left(\frac{294}{T_g}\right)^{0.25}$	Dent, 1971
Hiroyasu	$S = 0.39 \left(\frac{2\Delta P}{\rho_l}\right)^{0.5} t \quad 0 < t < t_b$ $S = 2.95 \left(\frac{\Delta P}{\rho_g}\right)^{0.25} (d_o t)^{0.5} \quad t > t_b$	Hiroyasu and Arai, 1990
Schihl	$S = 1.414 C_v^{0.5} \left(\frac{\Delta P}{\rho_g}\right)^{0.25} \left(\frac{d_o t}{\tan(\theta)}\right)^{0.5}$	Schihl *et al*., 1996
Naber and Siebers	$\tilde{S} = \left[\left(\frac{1}{\tilde{t}}\right)^n + \left(\frac{1}{\tilde{t}^{0.5}}\right)^n\right]^{\frac{-1}{n}}$	Naber and Siebers, 1996
Arrègle	$S = d_o^{0.307} \cdot P_{inj}^{0.262} \cdot \rho_g^{-0.406} \cdot t^{0.568}$	Arregle *et al*., 1999

spray penetration is a function of several engine operating parameters such as nozzle geometry, spray angle, injection conditions including the injection pressure, ambient density and temperature. The collected 0D spray tip penetration models are shown in Table 5.

1.2.1 Wakuri Model

Wakuri *et al*. (1960) used momentum theory to develop the fuel spray model by assuming that the relative velocity between fuel droplets and entrained air can be neglected and the injected liquid droplet momentum is transferred to the homogeneous fuel droplet-entrained air mixture for the density ratio range of 40-60. Their model is expressed by Equation (14):

$$S = 1.189 C_a^{0.25} \left(\frac{\Delta P}{\rho_g}\right)^{0.25} \left(\frac{d_o t}{\tan(\theta)}\right)^{0.5} \tag{14}$$

where C_a is the coefficient of contraction ($C_d = 1$ in this model), ΔP the difference between fuel injector pressure and ambient gas pressure, ρ_g the gas density, d_o the nozzle diameter and θ the spray angle.

1.2.2 Dent Model

Equation (15) of spray penetration is the jet mixing model, based on gas jet mixing theory, proposed by Dent (1971). This model is different from other models for considering the ambient temperature T_g effects by the term $(294/T_g)$:

$$S = 3.07 \left(\frac{\Delta P}{\rho_g}\right)^{0.25} (d_o t)^{0.5} \left(\frac{294}{T_g}\right)^{0.25} \tag{15}$$

1.2.3 Hiroyasu Model

Hiroyasu and Arai (1990) proposed Equations (16) and (17), which are derived from data obtained during the investigation (Hiroyasu *et al*., 1978) and from applying the jet disintegration theory by Levich (1962). They used two different equations, one from the beginning of the injection to the jet break-up time, where the penetration is proportional to time. The other occurs at times exceeding the jet break-up time, where the penetration is proportional to the square root of time:

$$S = 0.39 \left(\frac{2\Delta P}{\rho_l}\right)^{0.5} t \quad 0 < t < t_b \tag{16}$$

$$S = 2.95 \left(\frac{\Delta P}{\rho_g}\right)^{0.25} (d_o t)^{0.5} \quad t > t_b \tag{17}$$

where t_b is the jet break-up time, which can be evaluated by Equation (18):

$$t_b = 28.65 \frac{\rho_l d_o}{(\rho_g \Delta P)^{0.5}} \tag{18}$$

1.2.4 Schihl Model

Schihl *et al*. (1996) analyzed the existing spray penetration models and proposed the following phenomenological cone penetration model:

$$S = 1.414 C_v^{0.5} \left(\frac{\Delta P}{\rho_g}\right)^{0.25} \left(\frac{d_o t}{\tan(\theta)}\right)^{0.5} \tag{19}$$

1.2.5 Naber and Siebers Model

Equation (20) is a correlation given in Appendix C of Naber and Siebers (1996):

$$\tilde{S} = \left[\left(\frac{1}{\tilde{t}}\right)^n + \left(\frac{1}{\tilde{t}^{0.5}}\right)^n\right]^{\frac{-1}{n}} \tag{20}$$

where $\tilde{S}$ is the dimensionless penetration, $\tilde{t}$ the dimensionless time and n a model constant ($n = 2.2$):

$$\tilde{S} = \frac{S}{x^+} \tag{21}$$

$$\tilde{t} = \frac{t}{t^+} \tag{22}$$

where t^+ and x^+ are the time scale and length scale respectively, they are defined by Equations (23) and (24):

$$x^+ = \frac{C_a^{0.5} d_o \sqrt{\frac{\rho_l}{\rho_g}}}{\tan(\theta)} \tag{23}$$

$$t^+ = \frac{C_a^{0.5} d_o \sqrt{\frac{\rho_l}{\rho_g}}}{\tan(\theta) V_{inj}} \tag{24}$$

1.2.6 Arrègle Model

Arrègle *et al*. (1999) used a simple equation with different coefficients which have been fitted with experimental results on a Diesel spray. This equation depends only on the nozzle diameter, the injection pressure, the gas density and the time. This is the result:

$$S = d_o^{0.307} \cdot P_{inj}^{0.262} \cdot \rho_g^{-0.406} \cdot t^{0.568} \tag{25}$$

where P_{inj} is the injection pressure. We can observe that the spray penetration is proportional to a value close to the square root of the time, as in the other models.

1.2.7 Analysis and Validation

The data come from the same experiment that previously for the spray angle. The start of injection is defined as the first mass leaving the nozzle.

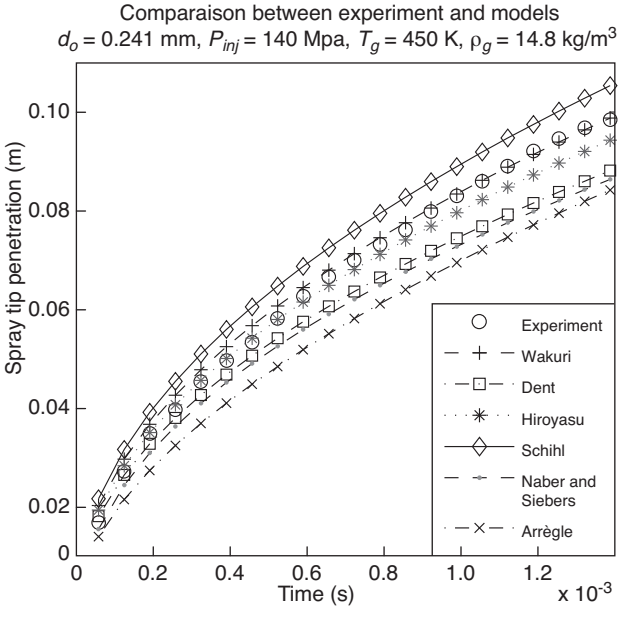

Figure 5

Example of 0D results for spray tip penetration.

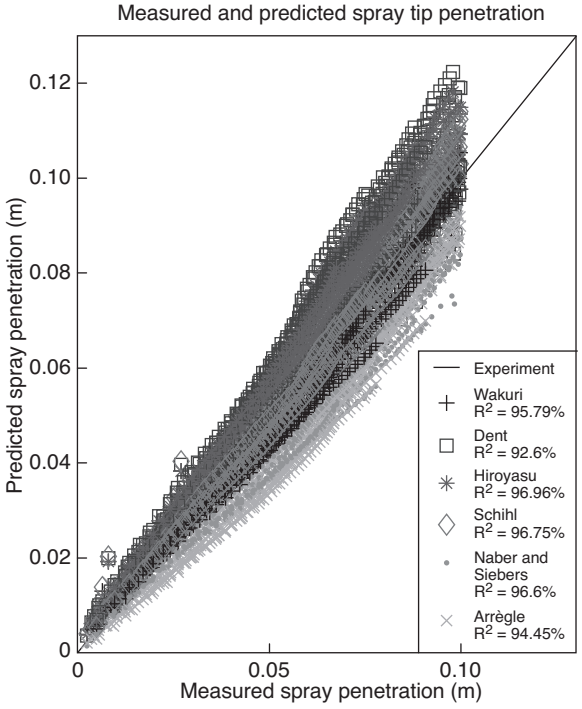

Figure 6

Comparison between measured and predicted spray tip penetration.

Figure 5 shows predicted and measured spray tip penetrations for one example. The shape of penetration is similar for all the models because they are all proportional to the square root of time. Concerning the break-up time t_b used by Hiroyasu, it has an influence on the first part of the penetration, until a value comprised between $4 \cdot 10^{-5}$ and $4 \cdot 10^{-4}$ seconds in our case.

In Figure 6 are represented 1 040 points (from 27 penetrations) for each model. All the models seem to be predictive.

The coefficient of determination and the mean absolute percentage error for each model are given in Table 6 (the best

TABLE 6

Comparison results between models and data

Spray angle model	Coefficient of determination	Mean absolute percentage error
Wakuri	95.79%	**7.57%**
Dent	92.60%	11.14%
Hiroyasu	**96.96%**	12.61%
Schihl	96.75%	8.77%
Naber and Siebers	96.60%	15.26%
Arrègle	94.45%	17.86%

values are in bold). In our case, Wakuri model gives a spray tip penetration value closed to the measured one. But the best prediction is given by Hiroyasu model. Also, the additional term with the ambient temperature, in Dent model equation, seems to reduce its validity.

1.3 Liquid Length Models

The purpose of this study is to investigate the applicability of the existing 0D liquid length models for spray. The collected spray angle models are show in Table 7.

TABLE 7

Different correlations for liquid length

Type of model	Correlation	References
Chehroudi	$L_b = Cd_o\left(\frac{\rho_l}{\rho_g}\right)^{0.5}$	Chehroudi *et al*., 1985
Beale and Reitz	$L_b = 0.5B_1 d_o\left(\frac{\rho_l}{\rho_g}\right)^{0.5}$	Beale and Reitz, 1999
Hiroyasu and Arai	$L_b = 7.0d_o\left(1+0.4\frac{r_o}{d_o}\right)\left(\frac{P_g}{\rho_l V_{inj}^2}\right)^{0.05}\cdot\left(\frac{l_o}{d_o}\right)^{0.13}\left(\frac{\rho_l}{\rho_g}\right)^{0.5}$	Hiroyasu and Arai, 1990
Siebers	$L_b = \frac{b}{a}\left(\frac{\rho_l}{\rho_g}\right)^{0.5}\frac{d_o C_a^{0.5}}{\tan(\theta)}\sqrt{\left(\frac{2}{B}+1\right)^2-1}$	Siebers, 1999
Enhanced model	$L_b = 93\left(\frac{294}{T_g}\right)^{1.43}\cdot d_o\left(\frac{\rho_l}{\rho_g}\right)^{0.5}$	-

1.3.1 Chehroudi Model

The more famous and simple equation for the liquid length expresses the fact that the core length is dependent on the ratio of liquid and gas density and that it is directly proportional to the nozzle hole diameter:

$$L_b = Cd_o\left(\frac{\rho_l}{\rho_g}\right)^{0.5} \quad (26)$$

where d_o is the nozzle diameter, ρ_l the liquid density and ρ_g the gas density. C is an empirical constant which expresses the influence of the nozzle flow conditions and other effects that cannot be described in detail. Chehroudi *et al*. (1985) performed some experiments and proposed that the constant C should be in the range 7-16. However, for our experiments, a value of 16.3 gives the best result.

1.3.2 Beale and Reitz Model

Beale and Reitz (1999) proposed a modified equation of the previous model:

$$L_b = 0.5B_1 d_o\left(\frac{\rho_l}{\rho_g}\right)^{0.5} \quad (27)$$

where B_1 is the well known breakup constant of Kelvin Helmholtz model. According with Su *et al*. (1996), this constant can be set to 60.

1.3.3 Hiroyasu and Arai Model

The following equation was given by Hiroyasu and Arai (1990) for the liquid length from experimental data which covered a wide range of conditions:

$$L_b = 7.0d_o\left(1+0.4\frac{r_o}{d_o}\right)\left(\frac{P_g}{\rho_l V_{inj}^2}\right)^{0.05}\left(\frac{l_o}{d_o}\right)^{0.13}\left(\frac{\rho_l}{\rho_g}\right)^{0.5} \quad (28)$$

where L_b is the liquid length, r_o is the radius of inlet edge of hole, P_g the ambient gas pressure, V_{inj} the injection velocity, l_o the length of the nozzle hole and ρ_g the gas density.

This equation includes the effect of the inlet edge rounding which shifts the inception of cavitation and turbulence to higher injection pressures and increases the liquid length. The influence of cavitation and turbulence is also included via the term $(P_g/\rho_l V_{inj}^2)$.

1.3.4 Siebers Model

Siebers (1999) has developed a scaling law to predict the liquid length. The assumptions made include quasi-steady flow with a uniform rate, uniform velocity, uniform fuel concentration and uniform temperature profiles (perfect mixing inside the spray boundaries), and finally no velocity slip between the injected fuel and the entrained gas. The model equation is the following:

$$L_b = \frac{b}{a}\left(\frac{\rho_l}{\rho_g}\right)^{0.5}\frac{d_o C_a^{0.5}}{\tan(\theta)}\sqrt{\left(\frac{2}{B}+1\right)^2-1} \quad (29)$$

where a and b are two constants (0.66 and 0.41 respectively) and θ the spray angle. B is the ratio of the fuel and ambient gas mass flow rates resulting in complete vaporization of the fuel:

$$B = \frac{Z_g\left(T_s, P_g - P_s\right)\times P_s \times M_l}{Z_l\left(T_s, P_s\right)\times\left[P_g - P_s\right]\times M_g} = \frac{h_g\left(T_g, P_g\right) - h_g\left(T_s, P_g - P_s\right)}{h_l\left(T_s\right) - h_l\left(T_l, P_g\right)} \quad (30)$$

where Z is the compressibility factor, M the molecular weights, P the pressure, T the temperature and h the enthalpy. The subscript g, l and s represents the ambient gas, the vaporized liquid and the saturated liquid vapor condition at the liquid length respectively.

The unknown, T_s, can be solved iteratively, given the fuel and ambient gas properties and initial fuel and ambient gas conditions. Once determined, T_s defines B, as well as the pressures, temperatures, and enthalpies of the fuel and ambient gas at the liquid length location.

The term B given by Equation (30) is analogous to the mass and thermal transfer numbers used in droplet vaporization studies (Lefebvre, 1989). Furthermore, the method of solving for T_s is analogous to that used in determining the surface temperature of a vaporizing liquid droplet (Lefebvre, 1989).

1.3.5 Enhanced Model

Experimental data shows a correlation between liquid length and ambient temperature *(Fig. 8)*. Previous models don't take into account this phenomenon, except Siebers's model.

By using Chehroudi's model, an additional term can be added. The resulting enhanced model is expressed in Equation (31):

$$L_b = C_1 \left(\frac{294}{T_g} \right)^{C_2} \cdot d_o \left(\frac{\rho_l}{\rho_g} \right)^{0.5} \tag{31}$$

where T_g is the ambient gas temperature. C_1 and C_2 are two constants to determine by a linear regression method. In our case a value of 93 and 1.43 is chosen, respectively.

1.3.6 Analysis and Validation

The experiments are different to the previous ones; the ambient temperature T_g is increased (700 K to 1 300 K instead of 450 K). The nozzles characteristics are listed in Table 8.

TABLE 8

Characteristics of nozzles

Orifice diameter	Discharge coefficient	Area-contraction coefficient		Length-to-diameter
d_o (mm)	C_d	C_a for 72 Mpa	C_a for 138 Mpa	l_o/d_o
0.100	0.80	0.91	0.86	4.0
0.180	0.77	0.85	0.82	4.2
0.251	0.79	0.88	0.79	2.2
0.246	0.78	0.89	0.81	4.2
0.267	0.77	0.89	0.82	8.0
0.363	0.81	-	0.85	4.1
0.498	0.84	0.94	0.88	4.3

The fuel is 2,2,4,4,6,8,8 heptamethylnonane ($C_{16}H_{34}$), with a density $\rho_l = 689$ kg/m^3 for a temperature $T_l = 436$ K. The percentage of oxygen is set to 0%, in order to disable combustion.

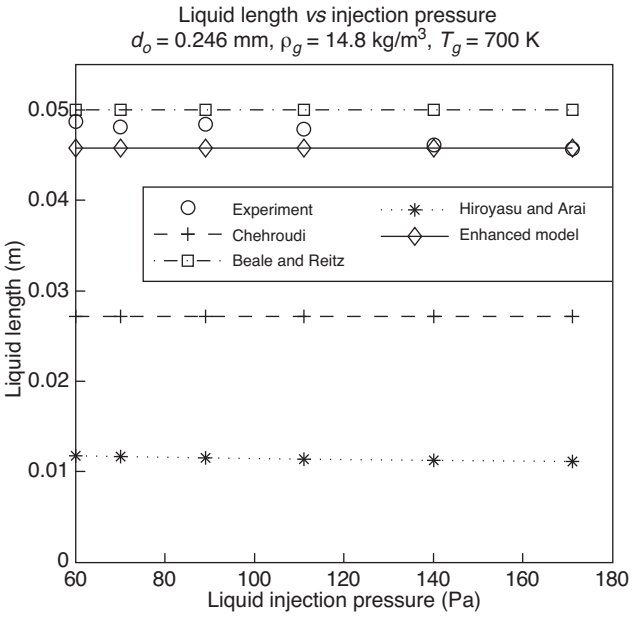

Figure 7

Evolution of liquid length with the injection pressure.

All the models include a density ratio in their equations, so their prediction for a variation of density is roughly the same. But concerning the injection pressure, only one model includes it (Hiroyasu and Arai model, indirectly with the injection velocity V_{inj} in the cavitation term ($P_g/\rho_l V^2_{inj}$)). Figure 7 shows that the liquid length decreases when the injection pressure rises, and Hiroyasu and Arai model predicts very well this phenomenon.

Concerning the ambient temperature, its effect is to decrease the liquid length when it rises. The phenomenon, shown in Figure 8, is well predicted by the enhanced model.

The coefficient of determination and the mean absolute percentage error for each model are given in Table 9 (the best values are in bold). The coefficient of determination is very low for the first models because the ambient temperature is not taken into account. The enhanced model is clearly more predictive with its additional term.

TABLE 9

Comparison results between models and data

Spray angle model	Coefficient of determination	Mean absolute percentage error
Chehroudi	54.78%	23.30%
Beale and Reitz	54.78%	70.41%
Hiroyasu and Arai	51.33%	61.51%
Enhanced model	98.06%	6.07%

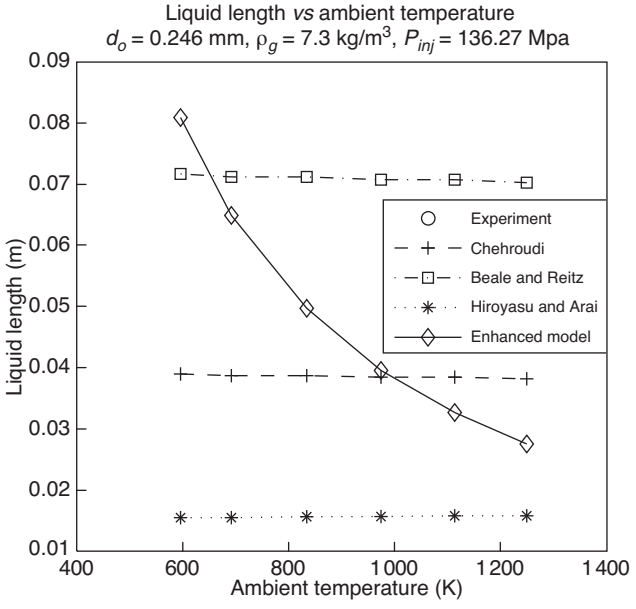

Figure 8

Evolution of liquid length with the ambient temperature.

Experiments used ambient conditions similar to the ones in an engine combustion chamber, and the injector is also comparable to the ones used in car engines. So our values of the constant C_1 and C_2 should be a good start in order to model the liquid length in an internal combustion engine.

1.4 Global Sauter Mean Diameter Models

The global Sauter Mean Diameter (SMD or $\overline{x}_{32}$) characterizes a single droplet with the same volume to surface area ratio as the ratio of the respective quantities integrated over the whole droplet size distribution present in a real spray:

$$\overline{x}_{32} = \frac{\sum_{i=1}^{N_{drops}} d_i^3}{\sum_{i=1}^{N_{drops}} d_i^2} \tag{32}$$

The SMD is a quantity characterizing the average droplet size of a spray. Many studies and correlations describe the SMD depending on the distance to the nozzle or on the breaking type or phase (Wu and Faeth, 1995; Faeth, 1996; Lee *et al*., 2007).

Some global SMD models are listed in Table 10, but the available data, mostly obtained by time-resolved point measurements is not pertinent for comparison.

TABLE 10

Correlation of SMD for different models

Type of model	Correlation	References
Hiroyasu	$\overline{x}_{32} = 2.33 \cdot 10^{-3} \Delta P^{-0.135} \rho_g^{0.121} m_l^{0.131}$	Hiroyasu *et al*., 1989
Varde	$\overline{x}_{32} = 8.7 d_o \left(Re_l We_l\right)^{-0.28}$	Varde *et al*., 1984
Hiroyasu and Arai	$\overline{x}_{32} = max\left[\overline{x}_{32LS}, \overline{x}_{32HS}\right]$ $\overline{x}_{32LS} = 4.12 d_o Re_l^{0.12} We_l^{-0.75} \left(\frac{\mu_l}{\mu_g}\right)^{0.54} \left(\frac{\rho_l}{\rho_g}\right)^{0.18}$ $\overline{x}_{32HS} = 0.38 d_o Re_l^{0.25} We_l^{-0.32} \left(\frac{\mu_l}{\mu_g}\right)^{0.37} \left(\frac{\rho_l}{\rho_g}\right)^{-0.47}$	Hiroyasu and Arai 1990
Merrington and Richardson	$\overline{x}_{32} = \frac{500 d_o^{1.2} \nu_l^{0.2}}{V_{inj}}$	Merrington and Richardson, 1947
Elkotb	$\overline{x}_{32} = 3.085 \nu_l^{0.385} \sigma_l^{0.737} \rho_l^{0.737} \rho_g^{0.06} \Delta P_l^{-0.54}$	Elkotb, 1982

1.4.1 Hiroyasu Model

The following equation is an empirical expression for the SMD for typical Diesel fuel properties and for hole type nozzle given by Hiroyasu *et al*. (1989):

$$\overline{x}_{32} = 2.33 \cdot 10^{-3} \Delta P^{-0.135} \rho_g^{0.121} m_l^{0.131} \tag{33}$$

where ΔP is the difference between fuel injector pressure and ambient gas, ρ_g the gas density and m_l is the amount of fuel delivery.

1.4.2 Varde Model

Varde *et al*. (1984) related the SMD to the diameter of the injection nozzle in the following equation:

$$\overline{x}_{32} = 8.7 d_o \left(Re_l We_l\right)^{-0.28} \tag{34}$$

where d_o is the nozzle diameter, Re_l the Reynolds number and We_l the Weber number.

1.4.3 Hiroyasu and Arai Model

Hiroyasu and Arai (1990) studied more in detail the effects of various parameters on the SMD like ambient pressure, injection pressure or the nozzle characteristics. Dimensionless analysis leaded to the following experimental equations for a complete spray:

$$\overline{x}_{32} = max\left[\overline{x}_{32LS}, \overline{x}_{32HS}\right] \tag{35}$$

$$\bar{x}_{32LS} = 4.12 d_o Re_l^{0.12} We_l^{-0.75} \left(\frac{\mu_l}{\mu_g}\right)^{0.54} \left(\frac{\rho_l}{\rho_g}\right)^{0.18} \quad (36)$$

$$\bar{x}_{32HS} = 0.38 d_o Re_l^{0.25} We_l^{-0.32} \left(\frac{\mu_l}{\mu_g}\right)^{0.37} \left(\frac{\rho_l}{\rho_g}\right)^{-0.47} \quad (37)$$

where μ_l and μ_g are the dynamic viscosity of the liquid and the gas respectively.

1.4.4 Merrington and Richardson Model

The disintegration of liquid jets injected into stagnant air was studied empirically (Merrington and Richardson, 1947). Drop-size distribution curves were obtained by a stationary nozzle directed vertically downward in an enclosed spray tower. The pressure supply was held constant during each test run by using a pressure-regulated gas cylinder.

(Lefebvre, 1989) gives a revision of the Merrington and Richardson SMD correlation including the effect of orifice diameter on the resulting SMD. The correlation for SMD is provided in Equation (38):

$$\bar{x}_{32} = \frac{500 d_o^{1.2} \nu_l^{0.2}}{V_{inj}} \quad (38)$$

where ν_l is the kinematic viscosity of the liquid and V_{ing} the injection velocity.

1.4.5 Elkotb Model

Elkotb (1982) has developed a model that takes into account numerous properties of both liquid and gas. In the end, experimental formula provides:

$$\bar{x}_{32} = 3.085 \nu_l^{0.385} \sigma_l^{0.737} \rho_l^{0.737} \rho_g^{0.06} \Delta P_l^{-0.54} \quad (39)$$

where ΔP is measured in bar. SMD value is given in μm.

1.5 Conclusion on 0D Model

We have seen in this part some spray characteristics of sprays like tip penetration or spray angle. Several 0D models have been considered and analyzed, and the results of the comparisons with experimental data show that these characteristics can be accurately predicted, and thus the spray correctly described.

Despite not being as exact as multidimensional models, 0D models offer important advantages like their reduced simulation time as well as their low computational requirements. For that reason, these models can be useful when a large number of simulations is needed.

But like there is not a spatial discretization in these models, the interaction between spray and the flow or the walls can not be modeled. Also the ambient conditions are fixed (volume, temperature...). In order to describe a spray evolving in a combustion chamber, multidimensional models should are needed.

2 MULTIDIMENSIONAL MODEL: RANS AND LES

In this part are listed the actual multidimensional models and methods used to model sprays, some results are shown for the most popular methods.

2.1 RANS; Liquid is Pure Lagrangian

2.1.1 Primary Break-Up

The task of a primary break-up model is to determine the starting conditions of drops which penetrate into the chamber (initial drop size and its velocity components). These conditions are principally influenced by the flow conditions inside the nozzle.

Blob Method

The blob method, developed by Reitz and Diwakar (1987), is the most popular of the models because of its simplicity. It is assumed that a detailed description of the atomization and breakup processes within the primary breakup zone of the spray is not required. This method creates big spherical droplets *(Fig. 9)* with the same diameter (usually equal to the nozzle hole diameter), which are then subject to secondary break-up. The number of drops injected per unit time is determined from the mass flow rate and the conservation of mass gives the injection velocity of the blobs.

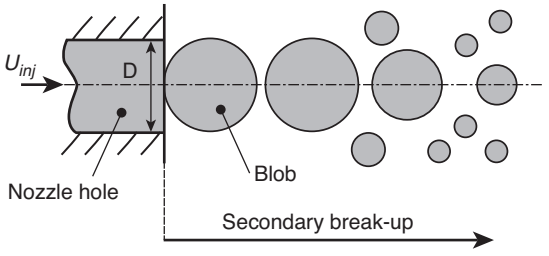

Figure 9

Blob method.

Kuensberg Sarre *et al.* (1999) suggested an enhanced version of the blob method. This method allows calculating an effective injection velocity and an effective injection particle diameter taking into account the reduction of the nozzle cross section due to cavitation (by decreasing the initial blob size and estimating a more realistic initial velocity).

Altogether, the blob methods are a good way to define the initial starting conditions for the liquid entering the chamber. But these methods do not represent a detailed physical and satisfying modeling of the relevant processes during primary break-up.

Distribution Functions

This method assumes that the fuel is already fully atomized at the nozzle exit and that the distribution of drop sizes can be described by mathematical functions. In this case, a distribution of droplet sizes is injected.

According to Levy *et al*. (1998), the droplet's diameter D at the nozzle exit should be sampled from a X^2-law in order to get a good agreement between measured and simulated downstream drop size distributions:

$$P(D) = \frac{1}{6\bar{D}^4} D^3 e^{-D/\bar{D}} \tag{40}$$

where $\bar{D} = SMD/6$. Various authors have used distribution functions in Diesel spray modeling like Long *et al*. (1994) and Lefebvre (1989).

It is also possible to predict the distribution function by using the Maximum Entropy Formalism (MEF) instead of a mathematical distribution function. Due to the use of a physically based criterion, the entropy of the distribution given by Shannon (1948), it is possible to estimate the most probable distribution function. Cousin and Desjonquères (2003) have used this method in order to predict drop size distributions in sprays from pressure-swirl atomizers.

Kelvin-Helmholtz Break-Up Model (KH Model)

The Kelvin-Helmholtz model (KH model or WAVE, *Fig. 10*) has been proposed by Reitz (1987). The model is based on a first order linear analysis of a Kelvin-Helmholtz instability growing on the surface of a cylindrical liquid jet that is penetrating into a stationary, inviscid and incompressible gas with a relative velocity.

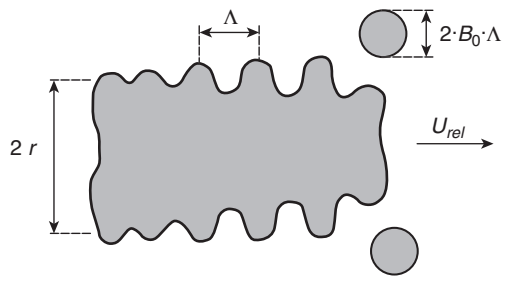

Figure 10

Illustration of the KH model.

From the solution of a general dispersion equation, maximum growth rate Ω_{KH} and corresponding wave length Λ_{KH} are given by the following equations:

$$\Omega_{KH}\left[\frac{\rho_l r_0^3}{\sigma}\right]^{0.5} = \frac{0.34 + 0.38 We_g^{1.5}}{(1+Z)(1+1.4T^{0.6})} \tag{41}$$

$$\frac{\Lambda_{KH}}{r_0} = 9.02\frac{(1+0.45Z^{0.5})(1+0.4T^{0.7})}{(1+0.87We_g^{1.67})^{0.6}} \tag{42}$$

where r_0 is the initial radius of the droplet, $Z = \sqrt{We_l}/Re_l$ and $T = Z\sqrt{We_g}$. The new radius of droplet r_{new} is given by:

$$r_{new} = 0.61\Lambda_{KH} \tag{43}$$

The new droplet continuously looses mass while penetration into the gas, its radius r is expressed in Equation (44):

$$\dot{r} = \frac{r - r_{new}}{\tau_{bu}} \tag{44}$$

$$\tau_{bu} = 3.788B_1\frac{r}{\Lambda_{KH}\Omega_{KH}} \tag{45}$$

where τ_{bu} is the characteristic time span.

Turbulence-Induced Break-Up

Huh and Gosman (1991) have published a model of turbulence-induced atomization for full-cone Diesel sprays. They assume that the turbulent forces within the liquid emerging from the nozzle are the producers of initial surface perturbations, which grow exponentially due to aerodynamic forces and form new droplets.

The droplets break up with a characteristic atomization length scale L_A and time scale τ_A. The characteristic atomization length is proportional to the turbulent length scale L_t:

$$L_A = C_1 L_t = C_2 L_w \tag{46}$$

where L_w is the wavelength of surface instability, determined by turbulence. According with the authors, C_1= 2 and C_2= 0.5. The characteristic atomization time scale τ_A can be calculated under the assumption that the time scale of atomization is a linear combination of the turbulence time scale τ_t and the wave growth time scale τ_w:

$$\tau_A = C_3\tau_t + C_4\tau_w = \tau_{spn} + \tau_{exp} \tag{47}$$

where $C_3 = 1.2$ and $C_4 = 0.5$. τ_{spn} and τ_{exp} indicate spontaneous wave growth time and exponential growth time.

This model shows good agreement with available experimental data for the spray cone angle of steady-flow single-hole experiments, but the effects of cavitation are not included.

Cavitation-Induced Break-Up

Arcoumanis and Gavaises (1997) have presented a primary break-up model that takes into account cavitation, turbulence, and aerodynamic effects. The initial droplet diameter is set equal to the effective hole diameter (blob method), and the first break-up of these blobs is modeled using the Kelvin-Helmholtz mechanism in the case of aerodynamic-induced break-up, the previous model of Huh and Gosman (1991) for turbulence-induced break-up, and a new phenomenological model in the case of cavitation-induced break-up.

The cavitation bubbles are transported to the blob surface by the turbulent velocity inside the liquid and either burst on the surface or collapse before reaching it, depending of the characteristic time scale. The radius of the bubbles is given by the following equations:

$$r_{cav} = \sqrt{r_0^2 - r_{eff}^2} \tag{48}$$

$$r_{eff} = \sqrt{\frac{A_{eff}}{\pi}} \tag{49}$$

where r_{cav} is the radius of bubble, r_{eff} the effective radius and A_{eff} is the effective area. The characteristic time scales for collapse τ_{coll} and bursting of bubbles τ_{burs} are:

$$\tau_{coll} = 0.9145 r_{cav} \sqrt{\frac{\rho_l}{\rho_{g,bubble}}} \tag{50}$$

$$\tau_{burst} = \frac{r_0 - r_{cav}}{u_{turb}} \tag{51}$$

where u_{turb} is the turbulent velocity ($u_{turb} = \sqrt{2k/3}$, k is the turbulent kinetic energy). The smaller characteristic time scale causes the break-up.

Cavitation and Turbulence-Induced Break-Up

Nishimura and Assanis (2000) have proposed a cavitation and turbulence-induced primary break-up model for full-cone Diesel sprays. During the injection period, discrete fuel parcels enter in the chamber with an initial diameter equal to the nozzle hole diameter. Each parcel contains bubbles *(see Fig. 11)*, according to the volume fraction and size distribution at the hole exit, computed from a phenomenological cavitation model inside the injector.

The authors assume that the velocity fluctuations inside the cylinder induce a deformation force on its surface:

$$F_{turb} = \text{surface dynamic pressure} = \pi D \frac{2D}{3} \frac{\rho_l}{2} u_{turb}^2 \tag{52}$$

It breaks up if the sum of F_{turb} and the aerodynamic drag force F_{aero} is no longer compensated by the surface tension F_{surf}:

$$F_{aero} = \pi \frac{2d_o^2}{3} 0.5 \rho_g u_{rel}^2 \tag{53}$$

$$F_{surf} = \pi D \sigma \tag{54}$$

The diameter of the original cylinder is reduced until $F_{turb} + F_{aero} = F_{surf}$ again.

2.1.2 Secondary Break-Up

Secondary break-up is the disintegration of already existing droplets into smaller ones due to the aerodynamic forces. These forces are induced by the relative velocity between droplet and surrounding gas. The result is an unstable growth of waves on the droplet surface which finally leads to the disintegration of the droplet into new ones.

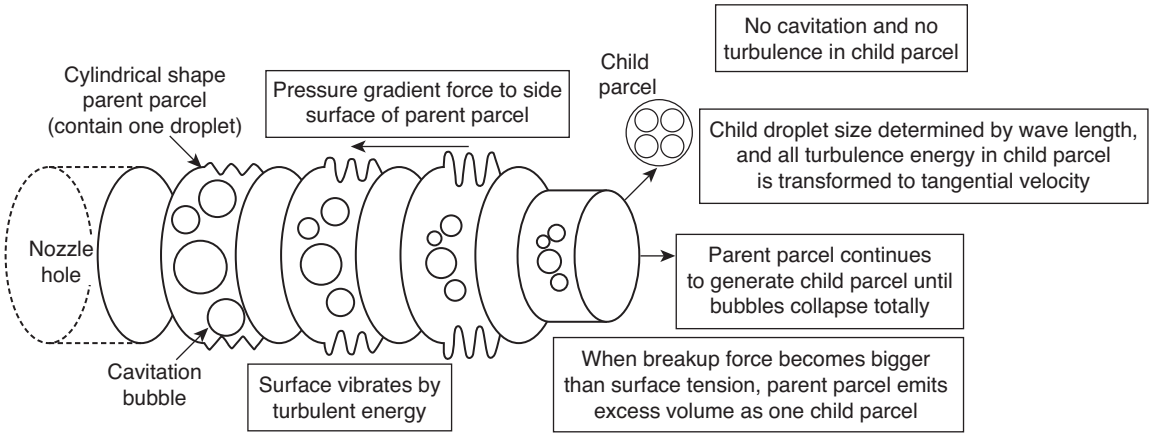

Figure 11

Primary break-up model of Nishimura and Assanis (2000).

Taylor-Analogy Break-Up Model (TAB Model)

The Taylor Analogy Break-up model was proposed by O'Rourke and Amsden (1987). It is based on an analogy between a forced oscillating spring-mass system and an oscillating and distorting droplet *(see Tab. 11)*.

TABLE 11

Comparison of a spring-mass system to a distorting droplet

Spring-mass system	Distorting and oscillating droplet
Restoring force of spring	Surface tension forces
External force	Droplet drag force
Damping force	Droplet viscosity forces

The deformation of the droplet is given by:

$$\ddot{y} = \frac{C_F}{C_b}\frac{\rho_g}{\rho_l}\frac{u_{rel}^2}{r^2} - C_k\frac{\sigma}{\rho_l r^3}y - C_d\frac{\mu}{\rho_l r^2}\dot{y} \tag{55}$$

where $C_f = 1/3$, $C_b = 0.5$, $C_k = 8$ and $C_d = 5$. u_{rel} is the relative velocity between droplet and gas and σ is the surface tension.

Tanner (1997) showed that the TAB model under predicts the droplets sizes of full cone sprays and has developed an enhanced version of this model (ETAB). The difference is that an initial oscillation is chosen for the spherical drops emerging from the nozzle (against no oscillation for TAB model).

Droplet Deformation and Break-Up Model (DDB Model)

Ibrahim *et al*. (1993) presented a droplet deformation and break-up model. It assumes that the liquid droplet is deformed from the initial spherical shape into an ellipsoidal one *(see Fig. 12)*.

The distortion of droplet that causes break-up is governed by the following equation:

$$K\ddot{y} + \frac{4N}{Re_g}\frac{1}{y^2}\dot{y} + \frac{27\pi^2}{16We_g}y\left[1 - 2\left(\frac{3\pi}{4}y\right)^{-6}\right] = \frac{3}{8} \tag{56}$$

where K is the liquid-gas density ratio and N is the liquid-gas viscosity ratio. The droplets start with zero deformation ($y = 4/3\pi$). The break-up happens when the deformation of droplet reaches the value given by:

$$\frac{a}{r} = \frac{We_g}{6\pi} \tag{57}$$

where a is the major semi-axis of the ellipsoidal cross section of the oblate spheroid.

The DDB and TAB model have a very similar breakup mechanism, so the DDB model can be regarded as an alternative to the TAB model.

Rayleigh-Taylor Break-Up Model (RT Model)

The Rayleigh-Taylor model (RT model, *Fig. 13*) is based on the theoretical work of Taylor (1950), who investigated the instability of the interface between two fluids of different densities in the case of an acceleration (or deceleration) normal to this interface.

From the assumption of linearized disturbance growth rates and negligible viscosity, the frequency of the fast-growing RT wave is given by:

$$\Omega_{RT} = \left(\frac{2}{3\sqrt{3\sigma}}\frac{\left[a\left(\rho_l - \rho_g\right)^{3/2}\right]}{\rho_l + \rho_g}\right)^{0.5} \tag{58}$$

The corresponding wavelength Λ_{RT} and wave number K_{RT} are given by:

$$\Lambda_{RT} = \frac{2\pi C_{RT}}{K_{RT}} \tag{59}$$

$$K_{RT} = \left(\frac{a\left(\rho_l - \rho_g\right)}{3\sigma}\right)^{0.5} \tag{60}$$

where a is the acceleration of the droplet and C_{RT} is a constant ($C_{RT} = 0.3$).

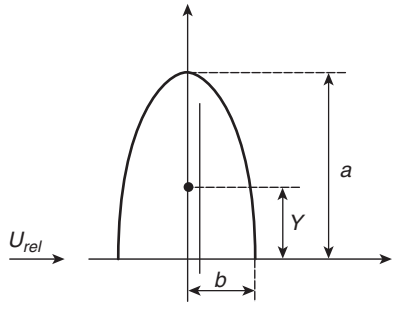

Figure 12

Schematic diagram of the deforming half drop.

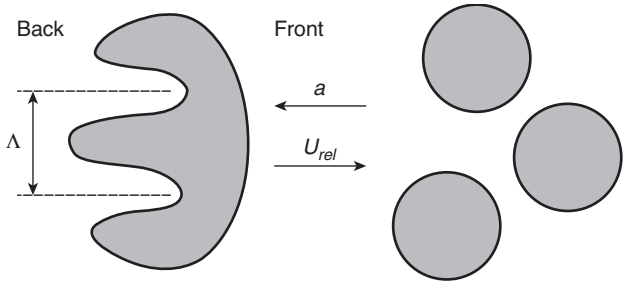

Figure 13

Illustration of the RT model.

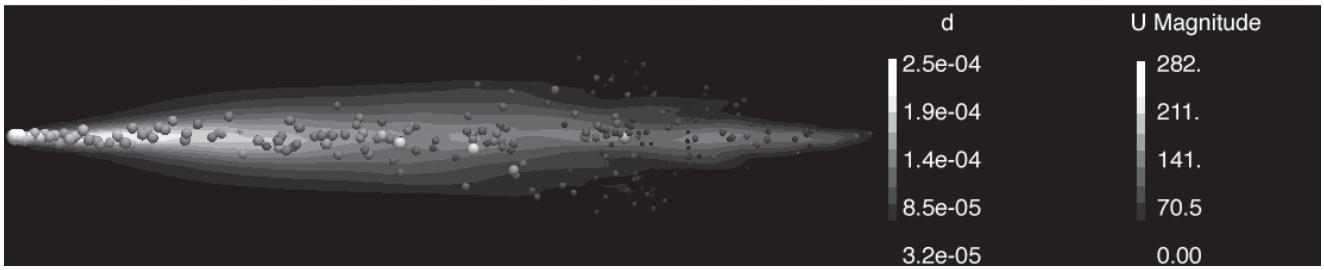

Figure 14

Lagrangian particles (color scale for diameter in meters) and Eulerian flow (color scale for velocities in m/s).

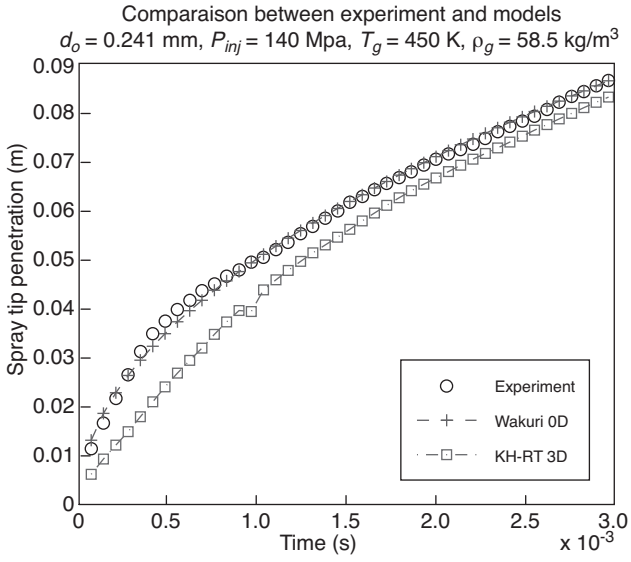

Figure 15

Penetration results for KH-RT Lagrangian particles in Eulerian flow.

If the corresponding wavelength is smaller than the droplet diameter, the instability of the RT wave increases. While the wave is growing, the wave growth time is tracked, and then compared with the break-up time. In RT break-up, the break-up time τ_{RT} and the radius after break-up r_{new} are defined by the following equations:

$$r_{new} = \frac{\pi C_{KH}}{K_{RT}} \tag{61}$$

$$\tau_{RT} = \frac{C_\tau}{\Omega_{RT}} \tag{62}$$

Combined Models

A single break-up model is usually not able to describe all break-up processes and break-up regimes of engine sprays. It is necessary to use combined models (usually a primary and a secondary break-up) in order to improve the accuracy of prediction.

Patterson and Reitz (1998) suggested the KH-RT hybrid breakup model with the concept that the competition between KH instability and RT instability causes the droplet breakup. Park *et al*. (2003) investigated the prediction accuracy of various hybrid models for high-speed Diesel fuel sprays and reported that the results of KH-RT model, KH-DDB model, and Turbulence-DDB model agree well with the experimental results.

2.1.3 Calculation

Figure 14 shows an example of utilization of the KH-RT model in order to model a Diesel high pressure spray. The software used is OpenFOAM 1.5-dev which includes natively the KH-RT model. The Lagrangian particles are injected in an Eulerian RANS flow using the k-ε turbulence model. Figure 15 is the penetration curve from 3D model compared to correlation and experimental data, showing a good agreement.

2.2 RANS; Liquid is Pure Eulerian

Wan and Peters (1999) developed an Eulerian approach from droplet equations, integrating over the radial direction to model Diesel sprays with a 1D model. Their ICAS (Interactive Cross sectional Averaged Spray) model is effective in simulating the vicinity of the nozzle up to the zone where the gas velocity becomes the predominant mixing mechanism. Vallet *et al*. (2001) and Beheshti and Burluka (2004) proposed a fully Eulerian spray atomization model by generalizing Kolmogorov hypothesis on turbulence to characteristic scales of spray. The principles of such modeling are currently used for the development of Eulerian-Lagrange coupled codes for spray simulation. The compressible Favre-averaged flow equations are applied to a single fluid with variable properties. The mass and momentum conservation

equations consider the contributions from one phase on another. The model is completed by k-ε equations for the two-phase turbulent kinetic energy (which includes kinetic energy in gas, liquid and the mean velocity gradient of the two phases) and dissipation rate, and then closed by an Algebraic Stress Model (ASM) of the Reynolds stress tensor. Specific treatment of atomizing liquid consists of conservation equation of liquid mean mass fraction:

$$\frac{\partial \overline{\rho}\tilde{Y}}{\partial t} + \frac{\partial \overline{\rho}\tilde{u}_i\tilde{Y}}{\partial x_i} = -\frac{\partial \overline{\rho}u_i{}'Y'}{\partial x_i} \tag{63}$$

with:

$$\frac{1}{\overline{\rho}} = \frac{\tilde{Y}}{\rho_l} + \frac{\left(1-\tilde{Y}\right)}{\rho_g} \tag{64}$$

and a state law:

$$\overline{p} = \frac{\rho\left(1-\tilde{Y}\right)r_g T_g}{1-\dfrac{\overline{\rho}\tilde{Y}}{\rho_l}} \tag{65}$$

along with a transport equation of mean interfacial area per unit volume:

$$\frac{\partial \overline{\Sigma}}{\partial t} + \frac{\partial \tilde{u}_i\overline{\Sigma}}{\partial x_i} = \frac{\partial\left(D_s \dfrac{\partial \overline{\Sigma}}{\partial x_i}\right)}{\partial x_i} + \left(A+a\right)\overline{\Sigma} - V_a\overline{\Sigma}^2 \tag{66}$$

$$\left(= \textit{diffusion} + \textit{production} - \textit{destruction}\right)$$

Diffusion term is written classically with a diffusion coefficient D_s that depends on turbulence and liquid fraction gradient. The production consists of two mechanisms, first is the action of velocity gradients that, according to a Kelvin-Helmholtz type instability, will stretch liquid-gas interface and make the surface larger. The author's choice is to give it a characteristic time A^{-1} equivalent to the one of turbulent kinetic energy production. The second is the action of turbulence which can also stretch and augment liquid-gas interface, with a characteristic time a^{-1} equivalent to the integral scale of turbulence. Last, the destruction term allows compensating production in such a way that at small scales, inertial forces be of the same order as surface tension: $We = 1$. The destruction term exponent being greater than 1, value of 2 is given to include the possibility of having two interfaces interacting inside a given volume.

In this approach, oriented towards large Reynolds and Weber number flows with a main velocity direction (hole injectors of Diesel type), surface tension, and viscosity are only effective at small scales, and where curvature and velocity gradients are important. At large scales, the characteristics of the flow are dependent only on fluid density. It is the generalization to atomization of Kolmogorov's results for turbulence. Also, it is possible to define in the same way, a critical scale of atomization where inertial forces balance surface tension:

$$We_c = \frac{\rho_c r_c u_c^2}{\sigma} \approx 1 \tag{67}$$

On the condition that balance between different processes of droplet formation of radius r_c (coalescence, break-up) and turbulent diffusion is obtained. Such a model includes some constants that can be tuned for solution. A correct calibration of the model can therefore lead to good simulation efficiency but the physical mechanisms of atomization are not explicitly represented resulting in the potential need for calibration of constants for each different case and hence limited generality.

2.3 RANS; Liquid is Eulerian-Lagrangian Represented

The Eulerian multiphase method can also be used for modeling the liquid in the near nozzle dense spray region combined to the Lagrangian method for zones where the spray is sufficiently diluted (far away from the nozzle). This method is called ELSA (Eulerian-Lagrangian Spray Atomization) and has been used by Demoulin *et al*. (2007) and Lebas *et al*. (2009).

2.4 LES; Liquid Fuel is Pure Lagrangian

Bharadwaj *et al*. (2009) have modeled an non-evaporative Diesel spray using the Lagrangian method with large eddy simulation. Their results show a good agreement. It was shown that a high speed Diesel spray can create significant energy at the sub-grid scale in the near nozzle region. This sub-grid kinetic energy is important in the models of sub-grid shear stress and droplet turbulent dispersion.

2.5 LES; Liquid Fuel is Pure Eulerian

Some studies have been to model a spray in full Eulerian in LES, like De Villiers *et al*. (2004). Their approach combines multiphase Volume-Of-Fluid (VOF) and large eddy simulation methodologies. It is used to perform quasi-direct transient fully three dimensional calculations of the atomization of a high-pressure Diesel jet, providing detailed information on the processes and structures in the near nozzle region, which is difficult to obtain by experimentation.

This methodology allows separate examination of diverse influences on the breakup process and is expected in due course to provide a detailed picture of the mechanisms that govern the spray formation. It is a powerful tool for assisting in the development of accurate atomization models for practical applications.

This approach has been used by Bianchi *et al*. (2007), who are also interested by the flow inside the nozzle which can influence the processes of atomization. In the case of

high-pressure injectors, cavitation can occur in the nozzle and changes the rest of the spray, Peng Karrholm *et al*. (2007) has worked on this phenomenon and has performed some calculations in order to model cavitation, with LES.

3 MULTIDIMENSIONAL MODEL: DNS

As classic simulations carry problematic issues concerning grid dependency, in order to correctly represent the spray, alternative solutions must be considered. The simplest is to carry direct numerical solutions. This of course can involve costly computer features if trying to solve the integral space domain. We propose here an alternative consisting on simulating only the very close vicinity of the spray and considering only the main processes in that region. For example, given the length and time scales, we do not consider evaporation (although some marginal and not precisely estimated amount of numerical "evaporation" is hard to avoid with the interface capturing techniques employed), Tomar *et al*. (2010). The idea is to carry independent simulations with varying parameters that can furnish adequate initial conditions (velocity, position and size of droplets) to spray models. Thus, DNS is carried up to the point where droplets reach a size small enough to be represented by Lagrangian particles. The principle has been studied and implemented by Tomar *et al*. (2010) based on GERRIS code by Popinet (2003), which has been applied to spray simulations (Fuster *et al*., 2009). When droplets reach a size small enough they are simply taken out from the fluid domain and implemented as Lagrangian particles. Balance of exchanges between droplets and gas is made for each cell, thus modifying gas flow.

Probably the main interest of DNS applied to spray consists on the possibility of modeling unsteady complex processes for which no validated models exist, for example the beginning of jet injection.

Simulations presented here are intended to explore the actual possibilities of the methodology. They are carried with an adaptive 3D mesh of a maximum of 2^9(512) cells per dimension when detailed aspects of liquid interface are required, or 2^7(128) when global quantities like penetration are estimated. With 2^9 cells the equivalent size of the smallest cells is 2.3 μm for an initial jet diameter of 0.2 mm, with 2^7 cells it is of 9.4 μm. The Reynolds and Weber number of experiments and simulations are theoretically 30 103 and 75 103 respectively although the effects of numerical viscosity and surface tension are still to be measured. Simulation results are therefore still to be validated and we only show here a comparison with spray penetration and qualitative aspects. Density ratio (gas/liquid) of simulation and experiments is . Results are presented in non-dimensional variables S^* and t^*:

$$S^* = \frac{S}{d_o} \tag{68}$$

$$t^* = \frac{t}{\left(\frac{d_o}{V_{inj}}\right)} \tag{69}$$

Figure 16 shows an example of the results obtained for the simulation of a pressure-hole type of spray at time $t^* = 20$ with the minimum mesh size, along with details of the adaptive mesh used by GERRIS code. The traced value is the iso-surface 0.5 for VOF tracer (0 is gas only, 1 is liquid only). Note that surface instabilities grow from inlet in a symmetric way due to meshing of the boundary conditions. They later develop into ligaments that ultimately form the droplets that detach and sub-divide. Although this can be considered as non-physical because dependent on meshing characteristics, surface instabilities growth are proven to be responsible for atomization. The real origin of such perturbations can be attributed to turbulence, roughness and other causes. Enhancement of such perturbations differs in a less iso-tropical distribution but growth depends on flow characteristics and relatively low on meshing. Globally, droplet and ligament formation is realistic. For computing time reasons droplets below a certain size have been removed. They can be treated in a Lagrangian way for full-spray calculations.

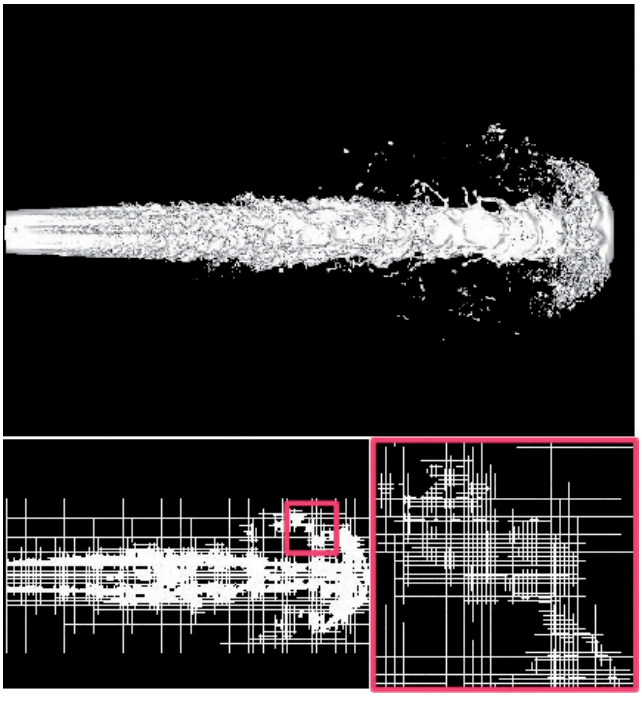

Figure 16

View of a pressure-hole type spray simulated by DNS with GERRIS code (top: VOF tracer 0.5 iso-surface), details of mesh in the cross section (bottom left) and of the squared zone (bottom right). Minimum cell size is $1/2^9$.

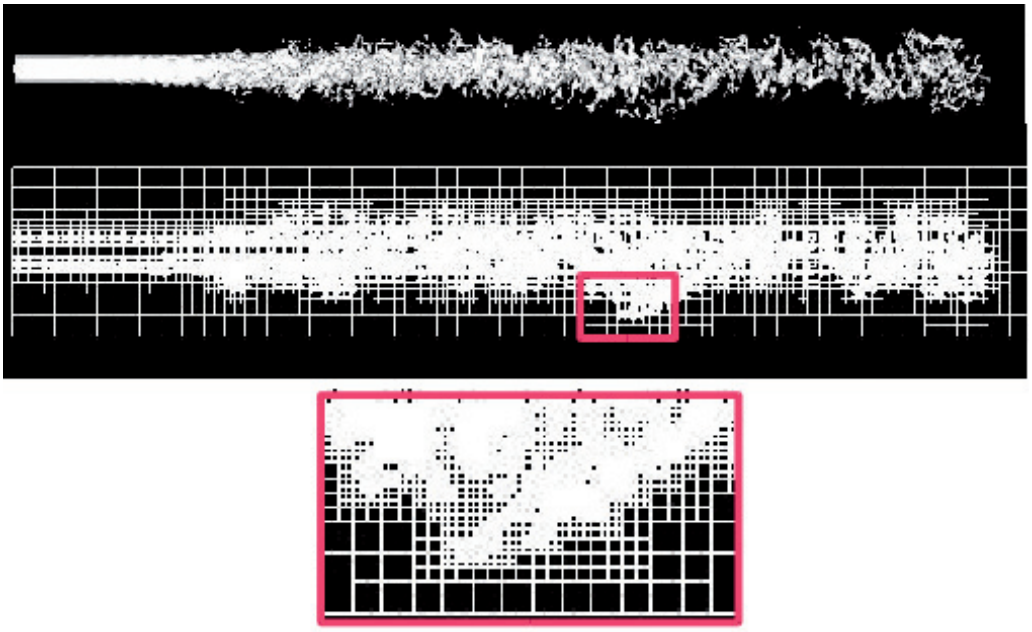

Figure 17

Spray aspect for non-dimensional time $t^* = 80$ (top: VOF tracer 0.5 iso-surface), corresponding mesh (middle) and detail of mesh (below). Minimum cell size is $1/2^7$.

In Figure 17, the same spray is represented at time $t^* = 80$ for a coarser mesh. Note that details on ligaments have not been lost although they are less refined. For values like penetration, the mesh change from 2^9 to 2^7 induces variations of less than 5%, for the time span we have tested. For later development of spray, as the liquid core vanishes, this observation may not remain valid.

In Figures (18-20), we show a comparison of simulation with images issued from experiments in similar conditions. Imaging is obtained through LIF of spray droplets with a four-hole injector (d_o = 0.2 mm) in a pressure vessel using iso-octane doped with fluoranthene as described in work by Le Moyne *et al*. (1997). Only one of the 4 sprays is correctly illuminated by the laser sheet intersecting it in its axis. A PIV set-up with a micro-telescope equipped camera is used. Figures 18 to 20 concern times t^* at 20, 40, and 80. In the experimental reference they correspond to 200, 400 and 800 microseconds after start of injection. The start of injection $t = 0$, is detected experimentally by the appearance of liquid at the nozzle hole.

Figure 21 shows a comparison of penetration for experimental and simulation data issued from a single simulation, showing good agreement. Low dispersion of this parameter has been verified for a limited set of simulations. Note that even for very early steps of spray development, penetration follows a power law. In this case:

$$S^* \propto \left(t^*\right)^{0.6772} \tag{70}$$

This is contrary to some assumptions made previously in literature, as no experimental data was available for so small times.

Simulation is carried removing all small droplets, so only the liquid core is represented here. Globally the general aspects of the liquid core are well captured by the simulation. Qualitatively the length scales of ligaments and droplets correspond to those of experiment images. As no effective method to measure droplet sizes in this very dense region of spray is available, a quantitative comparison of droplets sizes between simulation and experiments is not possible. Two representations of spray are shown with a cross section view of VOF tracer value and a 3D view of iso-surface at value 0.5 of VOF tracer. One can see that differences with experiments exist although no model for atomization or turbulence is implemented. One reason is that numerical aspects may not allow capturing the very complex interface. Another reason may be that boundary conditions for the simulation are not realistic.

Indeed, a parabolic velocity profile is injected into the simulation domain and break-up of droplets is not effective in the simulation until surface instabilities have grown enough. One can notice from experiment images that some atomization is visible from the very nozzle exit and that the smooth cylinder of simulations is not apparent in experiments.

The precocity of this atomization may be due to fastest growing instabilities or intra-hole phenomena. As the code is

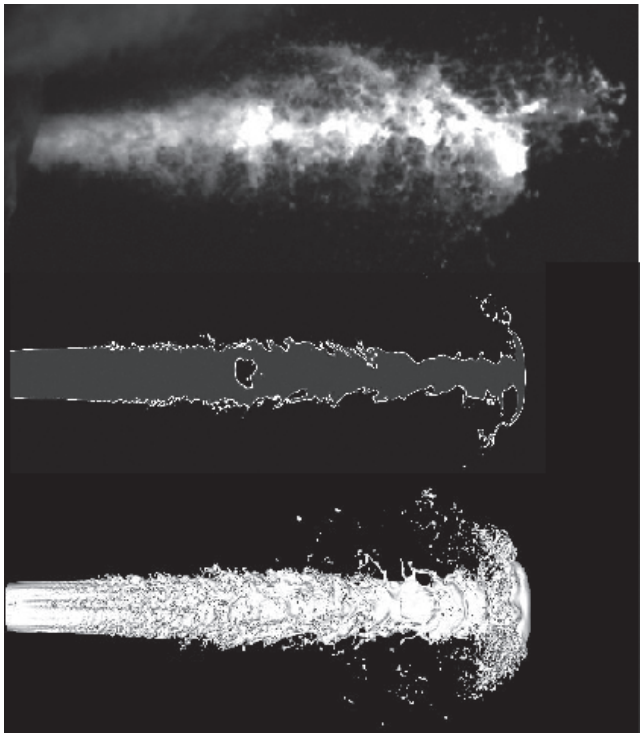

Figure 18

Spray image experiment and simulation at $t^* = 20$.

Figure 19

Spray image experiment and simulation at $t^* = 40$.

incompressible, and with no phase change for the time being, it is not possible to model cavitation-like mechanisms. However, as shown in Figure 22, by solving the 3D flow inside the injector it is possible to induce early atomization, namely from $t^* \sim 3$. This suggests that the velocity profile induced by complex flow inside the injector with vorticity sources, induced by rugosity for example, may play a role at least on early stages of atomization. Figure 23 shows a view

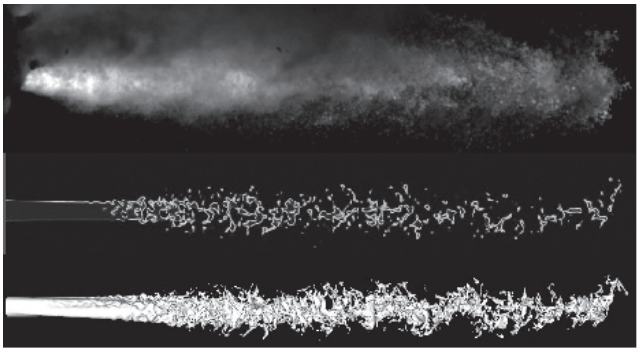

Figure 20

Spray image experiment and simulation at $t^* = 80$.

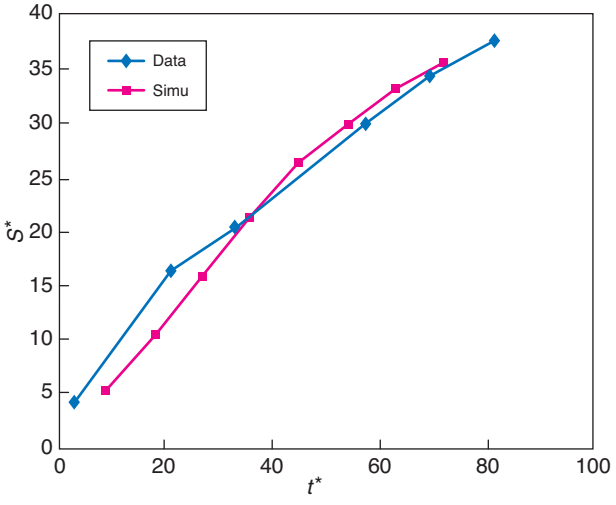

Figure 21

Non-dimensional penetration *versus* non-dimensional time for experiments and simulation.

of the spray at a very early stage of injection. The injection pressure has probably not reached its steady value as injector needle may still be moving. Expansion in the lateral directions and the corrugated aspect of the interface suggests that high levels of turbulence prevail from spray inception.

Further work is needed to validate the results and assumptions made, but as the DNS allows to capture the finest details of atomization it is, with the growing power of processors, a possible way to explore the spray formation mechanisms.

4 DISCUSSION

All the models cited in the previous sections show all the diversity of the results concerning spray formation. As the

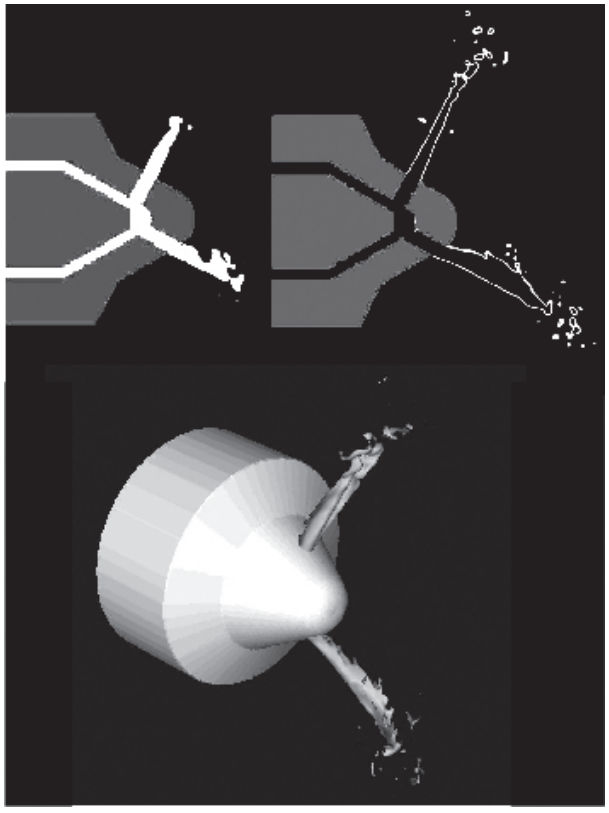

Figure 22

Example of DNS simulation for inter-injector flow (inside injector view left $t^* = 3$ and $t^* = 20$; and out-coming liquid right for $t^* = 20$).

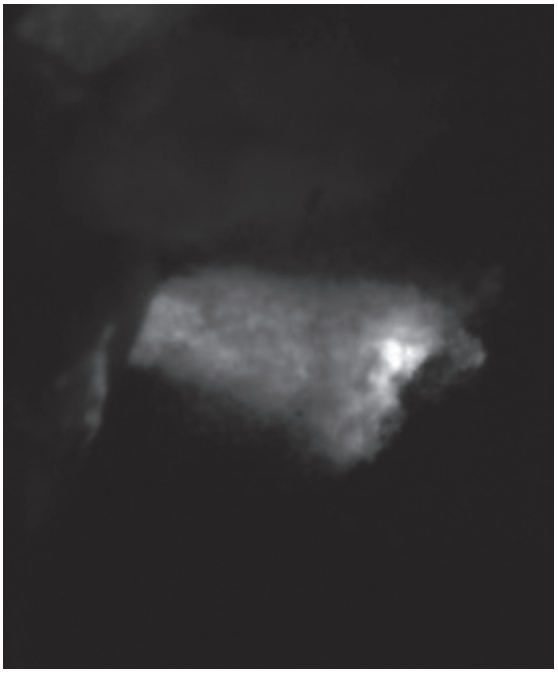

Figure 23

Early view of spray at $t^* = 3$.

process of atomization is of singular complexity the efforts to resume to few equations the effects of some parameters on strongly non-linear mechanisms give limited agreement with experiments. In the sense that when applied to different conditions to those where model constants and hypothesis were validated one often obtains non physical results. Every known spray model has a limited range of validity as quite different atomization regimes exist with a single device (Rayleigh regime, wind induced, atomization, flash boiling, effervescent atomization, etc.). Moreover, the experimental techniques available do not always allow access to necessary data like drop size and velocity in dense regions of spray. As a whole, when confronted to the need of simulating combustion processes in engines one often finds difficulties in choosing the correct spray sub-model and setting its several constants. Very often the final objective is completely reversed as a specific set of experiments is needed to calibrate the spray model. The semi-empirical correlations and 0D models have been extensively used and have proven their utility and limits. The widely spread use of Eulerian-Lagrangian models with RANS equations for gas phase has given relatively low valid results as the constants and parameters in spray models lack of a proven methodology for correct adjustment. Moreover, the issue of grid dependency, when addressed, asks difficult numeric questions at a certain computer cost. Finally, great hope is put on the LES and DNS simulations as the possibilities now at range allow starting to address the difficult points of spray modeling.

ACKNOWLEDGMENTS

Authors would like to thank Profs. Guibert and Zaleski, Danielson Engineering and Conseil Régional de Bourgogne for continuous support.

REFERENCES

Apte S.V., Gorokhovski M., Moin P. (2003) LES of Atomizing Spray with Stochastic Modeling of Secondary Breakup, *Int. J. Multiphase Flow* **29**, 1503-1522.

Arai M., Tabata M., Hiroyasu H., Shimizu M. (1984) Disintegrating Process and Spray Characterization of Fuel Jet Injected by a Diesel Nozzle, SAE International, *SAE paper* 840275.

Arcoumanis C., Gavaises M. (1997) Effect of Fuel Injection Processes on the Structure of Diesel Sprays, SAE International, *SAE paper* 970799.

Arrègle J.M., Pastor J.V., Ruiz S. (1999) The Influence of Injection Parameters on Diesel Spray Characteristics, SAE International, *SAE paper* 1999-01-0200.

Beale J.C., Reitz R.D. (1999) Modeling Spray Atomization with the Kelvin-Helmholtz/Rayleigh-Taylor Hybrid Model, *Atomization Sprays* **9**, 623-650.

Beheshti N., Burluka A. (2004) Eulerian Modelling of Atomisation in Turbulent Flows, *19th Annual Meeting of the Institute for Liquid Atomization and Spray Systems (Europe), Nottingham, 6-8 September,* 207-212.

Bharadwaj N., Rutland C., Chang S. (2009) Large Eddy Simulation Modelling of Spray-Induced Turbulence Effects, *Int. J. Engine Res.* **10**, 97-119.

Bianchi G. Minelli F., Scardovelli R., Zaleski S. (2007) 3D Large Scale Simulation of the High-Speed Liquid Jet Atomization, SAE International, *SAE paper* 2007-01-0244.

Chehroudi B., Chen S.-H., Bracco F.V., Onuma Y. (1985) On the Intact Core of Full-Cone Sprays, SAE International, *SAE paper* 850126.

Cousin J., Desjonquères P. (2003) A New Approach for the Application of the Maximum Entropy Formalism on Sprays, *ICLASS 2003, Sorrento, Italy, 13-17 July.*

De Villiers E., Gosman A., Weller H. (2004) Large Eddy Simulation of Primary Diesel Spray Atomization, SAE International, *SAE paper* 2004-01-0100.

Demoulin F.X., Beau P.A., Blokkeel G., Mura A., Borghi R. (2007) A New Model for Turbulent Flows with Large Density Fluctuations: Application to Liquid Atomization, *Atomization Sprays* **17**, 315-345.

Dent J.C. (1971) Basis for the Comparison of Various Experimental Methods for Studying Spray Penetration, SAE International, *SAE paper* 710571.

Elkotb M. (1982) Fuel Atomization for Spray Modelling, *Progr. Energ. Combust. Sci.* **8**, 61-90.

Faeth G. (1996) Spray Combustion Phenomena, *Symp. Int. Combust.* **26**, 1593-1612.

Fuster D., Bagué A., Boeck T., Moyne L.L., Leboissetier A., Popinet S., Ray P., Scardovelli R., Zaleski S. (2009) Simulation of Primary Atomization With an Octree Adaptive Mesh Refinement and VOF Method, *Int. J. Multiphase Flow* **35**, 550-565.

Heywood J. (1988) *Internal Combustion Engine Fundamentals*, McGraw-Hill.

Hiroyasu H., Arai M. (1990) Structures of Fuel Sprays in Diesel Engines, SAE International, *SAE paper* 900475.

Hiroyasu H., Arai M., Tabata M. (1989) Empirical Equations for the Sauter Mean Diameter of a Diesel Spray, SAE International, *SAE paper* 890464.

Hiroyasu H., Kadota T., Tasaka S. (1978) Study of the Penetration of Diesel, *JSME International Journal* **44**, 3208-3219.

Huh K.Y., Gosman A.D. (1991) A Phenomenological Model of Diesel Spray Atomization, *Proceedings of International Conference on Multiphase Flows, Tsukuba, Japan, 24-27 September.*

Ibrahim E.A., Yang H.Q., Przekwas A.J. (1993) Modeling of Spray Droplets Deformation and Breakup, *J. Propuls. Power* **9**, 651-654.

Kuensberg Sarre C., Kong S.C., Reitz R.D. (1999) Modeling the Effects of Injector Nozzle Geometry on Diesel Sprays, SAE International, *SAE paper* 1999-01-0912.

Le Moyne L. (2010) Trends in atomization theory, *Int. J. Spray Combustion Dynamics* **2**, 49-84.

Le Moyne L., Maroteaux F., Guibert P., Murat M. (1997) Model and Measure of Flows at the Intake of Engines, *J. Phys. III France* **7**, 1927-1940.

Lebas R., Menard T., Beau P., Berlemont A., Demoulin F. (2009) Numerical simulation of primary break-up and atomization: DNS and modelling study, *Int. J. Multiphase Flow* **35**, 247-260.

Lee K., Aalburg C., Diez F.J., Faeth G.M., Sallam K.A. (2007) Primary breakup of turbulent round liquid jets in uniform crossflows, *AIAA J.* **45**, 1907-1916.

Lefebvre H.A. (1989) *Atomization and Sprays*. Combustion: An International Series, Hemisphere, New-York, 434 p.

Levich V. (1962) *Physicochemical Hydrodynamics*, Prentice-Hall Inc., pp. 639-650.

Levy N., Amara, S., Champoussin J.C. (1998) Simulation of a Diesel Jet Assumed Fully Atomized at the Nozzle Exit, SAE International, *SAE paper* 981067.

Long W., Hosoya H., Mashimo T., Kobayashi K., Obokata T., Durst F., Xu T. (1994) Analytical Functions to Match Size Distributions in Diesel-Sprays, *International Symposium COMODIA, Yokohama, Japan, 11-14 July.*

Menard T., Beau P., Tanguy S., Demoulin F., Berlemont A. (2005) Primary break-up: DNS of liquid jet to improve atomization modelling, *WIT Transactions on Engineering Sciences* **55**, 343-352.

Merrington A.C., Richardson E.G. (1947) The break-up of liquid jets, *Proc. Phys. Soc.* **59**, 1.

Naber J.D., Siebers D.L. (1996) Effects of Gas Density and Vaporization on Penetration and Dispersion of Diesel Sprays, SAE International, *SAE paper* 960034.

Nishimura A., Assanis D.N. (2000) A Model for Primary Diesel Fuel Atomization Based on Cavitation Bubble Collapse Energy, *ICLASS 2000, Pasadena, CA, 16-20 July*, pp. 1249-1256.

O'Rourke P.J., Amsden A.A. (1987) The Tab Method for Numerical Calculation of Spray Droplet Breakup, SAE International, *SAE paper* 872089.

Park S.W., Lee C.S., Kim H.J. (2003) Investigation of Atomization Characteristics and Prediction Accuracy of Hybrid Models for High-Speed Diesel Fuel Sprays, SAE International, *SAE paper* 2003-01-1045.

Patterson M.A., Reitz R.D. (1998) Modeling the Effects of Fuel Spray Characteristics on Diesel Engine Combustion and Emissions, SAE International, *SAE paper* 980131.

Peng Karrholm F., Weller H., Nordin N. (2007) Modelling injector flow including cavitation effects for Diesel applications, *Proceedings of FEDSM2007 5th Joint ASME/JSME Fluids Engineering Conference, San Diego, CA, USA, 30 July - 2 August.*

Popinet S. (2003) Gerris: a tree-based adaptive solver for the incompressible Euler equations in complex geometries, *J. Computat. Phys.* **190**, 572-600.

Ranz W.E. (1958) Some Experiments on Orifice Sprays, *Can. J. Chem. Eng.* **36**, 175-181.

Reitz R. (1987) Modeling atomization processes in high pressure vaporizing sprays, *Atomization Sprays* **3**, 309-337.

Reitz R.D., Bracco F.B. (1979) On the Dependence of Spray Angle and Other Spray Parameters on Nozzle Design and Operating Conditions, SAE International, *SAE paper* 790494.

Reitz R.D., Diwakar R. (1987) Structure of High-Pressure Fuel Sprays, SAE International, *SAE paper* 870598.

Ruiz F., Chigier N. (1991) Parametric Experiments on Liquid Jet Atomization Spray Angle, *Atomization Sprays* **1**, 23-45.

Sandia National Laboratories (2010) online database, http://www.sandia.gov/ecn/cvdata/dsearch.php.

Schihl P., Bryzik W., Altreya A. (1996) Analysis of Current Spray Penetration Models and Proposal of a Phenomenological Cone Penetration Model, SAE International, *SAE paper* 960773.

Shannon C.E. (1948) A Mathematical Theory of Communication, *Bell Syst. Tech. J.* **27**, 379-423, 623-656.

Siebers D.L. (1999) Scaling Liquid-Phase Fuel Penetration in Diesel Sprays Based on Mixing-Limited Vaporization, SAE International, *SAE paper* 1999-01-0528.

Su T.F., Patterson M.A., Reitz R.D., Farrell F.V. (1996) Experimental and Numerical Studies of High Pressure Multiple Injection Sprays, SAE International, *SAE paper* 960861.

Tanner F.X. (1997) Liquid Jet Atomization and Droplet Breakup Modeling of Non-Evaporating Diesel Fuel Sprays, SAE International, *SAE paper* 970050.

Taylor G.I. (1950) The Instability of Liquid Surfaces When Accelerated in a Direction Perpendicular to their Planes, *Proc. R. Soc. London*, 192-196.

Tomar G., Fuster D., Zaleski S., Popinet S. (2010) Multiscale Simulations of Primary Atomization, *Comput. Fluids* **39**, 1864-1874.

Vallet A., Burluka A.A., Borghi R. (2001) Development of a Eulerian Model for the "Atomization" of a Liquid Jet, *Atomization and Sprays* **11**, 24.

Varde K.S., Popa D.M., Varde L.K. (1984) Spray Angle and Atomization in Diesel Sprays, SAE International, *SAE paper* 841055.

Wakuri Y., Fujii M., Amitani T., Tsuneya R. (1960) Studies of the Penetration of a Fuel Spray in a Diesel Engine, *JSME International Journal* **3**, 123-130.

Wan Y., Peters N. (1999) Scaling of Spray Penetration with Evaporation, *Atomization and Sprays* **9**, 111-132.

Wu P.-K., Faeth G. (1995) Onset and End of Drop Formation Along the Surface of Turbulent Liquid Jets in Still Gases, *Phys. Fluids* **7**, 2915-2917.

Final manuscript received in March 2011
Published online in September 2011